J Mater Sci (2013) 48:3138–3146
DOI 10.1007/s10853-012-7091-x

First-principles calculations of elastic moduli of Ti–Mo–Nb alloys using a cluster-plus-glue-atom model for stable solid solutions

Chong Zhang · Hua Tian · Chuanpu Hao · Jijun Zhao · Qing Wang · Enxue Liu · Chuang Dong

Received: 10 October 2012 / Accepted: 11 December 2012 / Published online: 19 December 2012

Abstract Using the first-principles calculations, a cluster-plus-glue-atom model was employed to investigate the elastic and electronic properties of Ti–Mo–Nb alloys with cluster formula of $[MoTi_{14}]$ (glue atom)$_x$ (glue atom = Ti, Mo, Nb, $x = 1$ or 3) for a theoretical guidance in composition design of β titanium alloys. The bulk modulus, shear modulus, Young's modulus, and Poisson ratio were evaluated from the calculated elastic constants using Voigt–Reuss–Hill average scheme on the periodic supercell model of cluster packing. The electronic properties of the Ti–Mo–Nb alloys were discussed by analyzing the electron density of state and Mulliken population. Meanwhile, we designed two series of Ti–Mo–Nb alloys, i.e., $[MoTi_{14}]X_1$ (X = Ti, Mo, Nb) and $[YTi_{14}]Nb_3$ (Y = Ti, Mo), and experimentally measured their mechanical properties. Our theoretical results (including mass density, Young's modulus, ductility) based on our cluster packing model agreed well with the experimental data, especially for $[TiMo_{14}]X_1$ (X = Ti, Mo, Nb) alloy series. On the contrary, the random solid solution structures were mechanically unstable and the calculated values significantly deviated from the experiments. Based on the cluster-plus-glue-atom model, an Ashby map of E/ρ versus B/G was constructed and indicated the inverse correlation between stiffness and ductility, for which the random solid solution model was unable to reflect. The Mo/Ti = 1/14 rule derived from the cluster model may serve as an important guideline for composition design of Ti–Mo based systems to achieve low elastic modulus alloys with stable β phase.

C. Zhang · H. Tian · C. Hao · J. Zhao · Q. Wang · E. Liu · C. Dong
Key Laboratory of Materials Modification by Laser, Ion and Electron Beams, Dalian University of Technology, Ministry of Education, Dalian 116024, China

C. Zhang · H. Tian · C. Hao · Q. Wang · E. Liu · C. Dong
School of Materials Science and Engineering, Dalian University of Technology, Dalian 116024, China

C. Zhang · H. Tian · J. Zhao (✉)
College of Advanced Science and Technology, Dalian University of Technology, Dalian 116024, China
e-mail: zhaojj@dlut.edu.cn

Introduction

β-Ti alloys have been one of the most attractive biomaterials due to their superior biocompatibility and mechanical properties, including relatively low elastic modulus with regard to the conventional materials like stainless steels and cobalt-based alloys [1–5]. Over the past few years, significant effort has been devoted to develop these bcc structural Ti-based alloys, and a few of them have already been implemented into biomedical applications [6]. They usually contain multiple non-toxic alloying elements, such as Mo, Nb, Ta, and Zr, which are preferred to as β stabilizers or/and play the key role in decreasing the Young's modulus [7–9]. To design these multi-component alloys, several methods were proposed like *d*-electrons concept [10] and Mo-equivalence method [11]. However, it is difficult to determine the optimum alloy composition with sufficiently stable β phase and enough low modulus which is generally achieved by multiple alloying of simple binary alloys. To design novel Ti-based alloys with desirable properties, it is necessary to develop a theoretical guidance in selecting suitable alloying elements.

The first-principles predictions based on density functional theory (DFT) have been used to simulate Ti-based materials and to provide theoretical guidance in composition design with respect to their crystalline structures and

elastic stiffness [12–14]. Previously, such DFT calculations have been performed to predict elastic constants and Young's modulus of titanium alloys for a set of binary systems, and negative Young's moduli for the bcc titanium alloys with high Ti concentrations were obtained [12]. Those calculations revealed a strong correlation between Young's modulus and atomic configuration. Ikehata et al. [13] systematically studied the $Ti_{1-x} - X_x$ (X = V, Nb, Ta, Mo, and W) binary alloys for $x = 0.0$, 0.25, 0.5, 0.75, 1.0 with a rigid band model to explore the possibility of realizing low Young's modulus in materials. Therefore, it is necessary to establish a correlation between composition/structure and mechanical properties of these alloys [10, 15]. Recently, our group proposed a composition rule for complex metallic alloys, named cluster-plus-glue-atom model considered the optimized nearest neighbor configuration. This model shows its potential capability in guiding composition design of a variety of industrial alloys [16, 17].

The relationship between phase stability and elastic properties will be treated in this paper in a consistent way, because it is an important criterion for developing Ti-based alloys for biomedical applications. Based on $MoTi_{14}$ cluster, our group recently designed a series of compositions for Ti-based alloys with stable β phase and the measured Young's moduli were about 50–100 GPa [18]. In this paper, we employed the cluster-plus-glue-atom model for stable solid solutions to describe the local atomic configurations and to design the optimized alloy compositions for Ti–Mo–Nb system with low Young's moduli and high bcc structural stabilities. The mechanical properties of these Ti–Mo–Nb alloys were investigated using the first-principles calculations as well as experimental measurements. The effects of short-range order of atomic arrangement on elastic properties were discussed by comparing with the random solid solution model. Our theoretical results based on the cluster-plus-glue-atom model are in line with the experimental data, which provide insightful guidance for composition design of β-Ti alloys.

Models and methods

Cluster formulae for stable Ti–Mo–Nb solid solutions

Within traditional crystallography, describing the structure of a complex metallic alloys is rather complicated since their essential structural characteristics are always submerged in a long list of atomic coordinates. Our group proposed a cluster-plus-glue-atom model to describe the structures of complex metallic alloys in terms of appropriate polyhedral units, which are referred to be the basic first coordination polyhedrons (namely, clusters) derived from the crystalline phases of relevant intermetallic compounds. In this model, the chemical composition of an phase can be expressed as the cluster formula: [cluster](glue atoms)$_x$ [19]. For example, based on the cluster line of Fe/Ni = 1/12, we proposed a cluster formula of $[FeNi_{12}]Cu_x$ to explain the solubility of Fe in Cu–Ni alloys [20]. Ab initio molecular dynamics simulations for binary $Cu_{64}Zr_{36}$ bulk metallic glass showed that the atomic structure of glass state was gradually dominated by icosahedral Cu_8Zr_5 cluster with decreasing temperature [21], which was predicted by the cluster formula of $[Cu_8Zr_5]Cu$ [22]. This model provides an alternative view of understanding the atomic arrangement in complex metallic alloys and establishes a bridge between local atomic structure and chemical composition of an alloy.

In a substitutional solid solution, it is suggested that the constituent elements with negative enthalpy of mixing ($\Delta H < 0$) prefer to form short-range order spherical atomic clusters. For bcc systems, Singh et al. [23] employed a Kanzaki lattice static method for evaluating the strain field induced by the substitutional transition metal impurities in vanadium matrix. Their results showed that the strain field was oscillatory in nature and concentrated in the region consisting of the first and second nearest neighbors, which formed a CN14 rhombic dodecahedron cluster. In Ti–Mo–Nb ternary system, Ti and Mo have a negative enthalpy of mixing ($\Delta H_{\text{Ti–Mo}} = -4$ kJ mol^{-1}); on the contrary, there is a small positive enthalpy of mixing ($\Delta H_{\text{Ti–Nb}} = 2$ kJ mol^{-1}) between Ti and Nb, suggesting that Ti atoms tend to stay close to Mo rather than Nb [24]. Thus, in our model, we propose a Mo-centered $MoTi_{14}$ rhombic dodecahedron cluster as the building block, which reflects the short-range interaction between solute and solvent elements in Ti-based Ti–Mo–Nb alloys, as shown in Fig. 1. An essential feature of our model for stable solid solution is the isolation of the clusters. According to the calculations by Singh et al. [23], sharing atoms between two CN14 rhombic dodecahedron clusters would induce overlap of strain field. Hence, it is reasonable to assume that these $MoTi_{14}$ clusters are distributed in the bcc crystal lattice in a separated manner and the glue atoms are placed on the lattice sites between the isolated clusters. These alloys can thus be represented by the cluster formula of $[MoTi_{14}]$(glue atom)$_x$.

The cluster formulae can successfully explain the known composition points. For Ti–Mo binary system, the cluster formula of $[MoTi_{14}]Mo = Ti_{87.5}Mo_{12.5}$ (at.%) is closely located at the critical monotectoid composition of $Ti_{88}Mo_{12}$ on the binary phase diagram [25]. If replacing the glue atom Mo by Ti, the cluster formula becomes $[MoTi_{14}]Ti = Ti_{93.75}Mo_{6.25}$ (at.%), closes to the experimentally achieved critical composition of $Ti_{94.75}Mo_{5.25}$ (Ti–10Mo in wt%) with stable β phase and the lowest Mo content [26]. Similarly, for Ti–Nb binary system, the

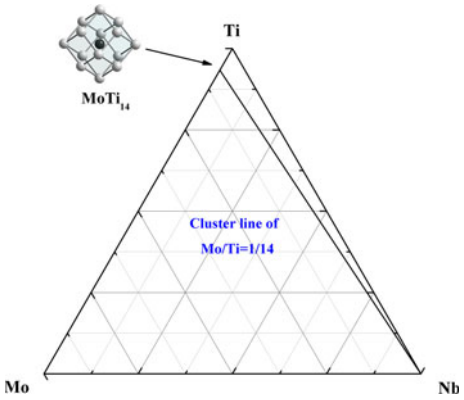

Fig. 1 Composition chart of Ti–Mo–Nb ternary phase diagram and cluster line of Mo/Ti = 1/14

cluster formula of $[TiTi_{14}]Nb_3 = Ti_{83.33}Nb_{16.67}$ (at.%) coincides with earlier experimental finding that Nb was able to stabilize the β phase at 16.98 at.% (Ti–28.4Nb in wt%) [25]. Though in principle, the clusters should be arranged in a random manner in the bcc lattice (otherwise a new crystalline phase would arise), periodic packing of isolated clusters has to be assumed in order to carry out the feasible first-principles calculations. Based on the above discussions, two series of Ti–Mo–Nb alloys, i.e., $[MoTi_{14}]X_1$ (X = Ti, Mo, Nb) and $[YTi_{14}]Nb_3$ (Y = Ti, Mo) are taken into account and the relevant cluster packing supercells are given in Fig. 2. As shown, the CN14 rhombic dodecahedron clusters efficiently fill the bcc lattice in a close-packed manner with glue atoms located in the interstitial sites between the clusters. The corresponding lattice constants are given in Table 1.

Experimental methods

Based on the cluster formula of $[MoTi_{14}](\text{glue atom})_x$ ($x = 1, 3$), we designed and fabricated two series of Ti–Mo–Nb alloys by changing the element species and the number of the glue atoms. Hence, the corresponding cluster formulae are $[MoTi_{14}]X_1$ (X = Ti, Mo, Nb) and $[MoTi_{14}]Nb_3$ alloys. These alloy samples were prepared from 99.99 wt% pure Ti, 99.99 wt% pure Mo, and 99.95 wt% Nb by arc melting in argon atmosphere. Button-shaped ingots were finally chill-cast into rod-shaped specimens with diameter of 3 mm and 6 mm in water-cooled copper molds. Some of the cast specimens were subjected to solution heat treatment (HT) at 1173 K for 2 h in Ar gas atmosphere and quenched with water to room temperature. In the following discussions of this paper, the copper mold suction casting alloys and the alloys by solution heat treatments are abbreviated to SC and HT alloys, respectively.

The mass densities of the alloy samples were determined by the Archimedean method. Mechanical properties, such as Young's modulus, were measured from tensile tests by MTS 810 material testing system, with a crosshead speed of 8.33×10^{-6} m s^{-1} at room temperature. The microstructures of the prepared Ti–Mo–Nb rods were characterized using OLYMPUS optical microscope and Bruker D8 Focus X-ray diffraction analyzer (Cu $K_{\alpha 1}$ radiation, $\lambda = 0.15406$ nm).

Computational methods

Parallel to the experimental synthesis and measurements, we performed the first-principles calculations within the framework of density functional theory (DFT) implemented in CASTEP software [27] to further validate our cluster-plus-glue-atom model and to gain deeper insight into these alloys. The interactions between ions and valence electrons were described by the ultrasoft pseudopotentials [28]. Exchange correlation interaction was described by the generalized gradient approximation with the revised Perdew, Burke, and Ernzerhof functional [29]. The energy cutoff was chosen as 350 eV. For each crystal structure, the equilibrium lattice constants and atomic coordinates were fully relaxed. Starting from the optimized crystal structures, full sets of elastic constants needed to

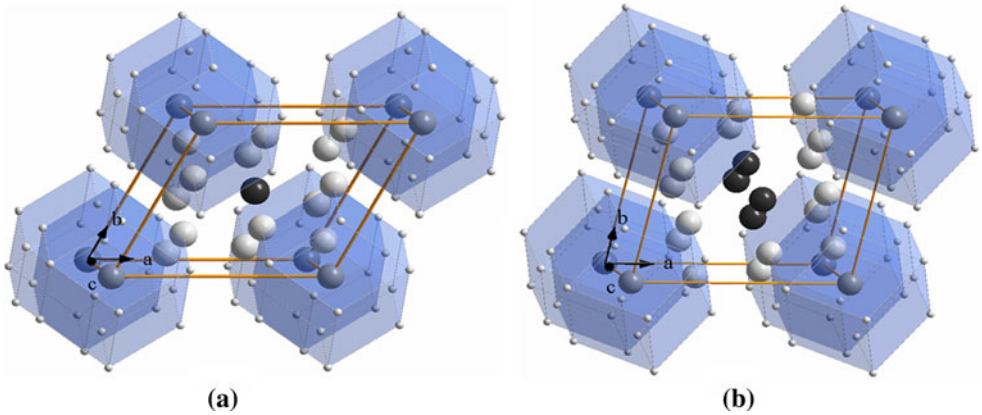

Fig. 2 Unit cells of the cluster packing structures. Atoms located on the vertex of each unit cells are the center atoms of CN14 clusters with *gray color*, while the *black ones* are glue atoms. The rest fourteen Ti atoms locate on the shells. The matched four $MoTi_{14}$ clusters are also given. **a** $[MoTi_{14}]X_1$ (X = Ti, Mo, Nb); **b** $[YTi_{14}]Nb_3$ (Y = Ti, Mo) alloy series

Table 1 Lattice constants of $[MoTi_{14}]X_1$ (X = Ti, Mo, Nb) and $[YTi_{14}]Nb_3$ (Y = Ti, Mo) alloy series, as experimentally measured bcc lattice constants, and the relevant values used for the cluster packing supercells

The a_{bcc} listed were obtained by XRD

Alloy	Experiment	Cluster packing structure					
	a_{bcc} (Å)	a (Å)	b (Å)	c (Å)	α	B	γ
$[MoTi_{14}]Ti$	3.26	7.30	7.11	7.11	61.73	72.07	59.14
$[MoTi_{14}]Mo$	3.27	7.31	7.13	7.13	61.73	72.07	59.14
$[MoTi_{14}]Nb$	3.27	7.31	7.13	7.13	61.73	72.07	59.14
$[TiTi_{14}]Nb_3$	3.28	7.14	7.14	7.14	61.73	86.98	80.92
$[MoTi_{14}]Nb_3$	3.28	7.14	7.14	7.14	61.73	86.98	80.92

calculate the isotropic properties were obtained by stress–strain method. The elastic constants are defined by means of solving linear equation sets of the stress–strain relationship with a certain path.

With the elastic constants from DFT calculations, the bulk modulus (B) and isotropic shear modulus (G) for polycrystalline crystals were evaluated by means of Voigt–Reuss–Hill average scheme [30]. Once B and G values are known, the polycrystalline (isotropic) Young's modulus (E) and Poisson ratio (v) of the alloy can be simply calculated according to the following relationship: $E = 9BG/(3B + G)$ and $v = (3B - E)/6B$. In addition, two essential engineering parameters to quantify ductility and stiffness of a material, i.e., the ratio of bulk modulus to shear modulus (B/G) [31] and the specific modulus of Young's modulus to mass density (E/ρ) were also calculated.

Within the cluster-plus-glue-atom model, we investigated $[MoTi_{14}]X_1$ (X = Ti, Mo, Nb) and $[YTi_{14}]Nb_3$ (Y = Ti, Mo) alloy series using the first-principles scheme described above. To elucidate the effects of short-range order on the mechanical properties, we also constructed a series of supercell models for random solid solutions of $MoTi_{14}X_1$ (X = Ti, Mo, Nb) and $MoTi_{15-x}Nb_x$ (x = 1, 2, 3) alloys. Each simulation supercell consists of 2 × 2×2 bcc unit cells with totally 16 atoms. According to the previous study, both thermodynamic stability and elastic properties of binary β-Ti alloys could be well predicted using cubic supercells with totally 16 atoms based on the first-principles calculations [12]. The structures of random solid solution can be modeled by different methods, such as special quasi-random structure [32]. As discussed above within the frame of cluster-plus-glue-atom model, the low levels of Mo and Nb combined with the effect of enthalpy of mixing show that Ti tend to stay close to Mo rather than Nb, which is taken into account to construct the random solid solution model in this work. In our modeled random structures, Mo and Nb tend to be separated by Ti atoms in our random solid solution model. For each composition, a few random configurations are generated and their physical properties are also presented in the discussions. The final alloy compositions for both cluster model and random model for these solid solutions are listed in Table 2.

Results and discussion

Elastic properties of $[MoTi_{14}]X_1$ and $[YTi_{14}]Nb_3$ alloys

The elastic constants of $[MoTi_{14}]X_1$ (X = Ti, Mo, Nb) alloy series are first investigated by both experiments and the first-principles calculations. According to our XRD experiments, all $[MoTi_{14}]X_1$ alloys consist of stable β phase at room temperature, as shown in Fig. 3. This is in line with the earlier experimental finding that Mo was an effective β stabilizer and 5 at.% of Mo was enough to stabilize β phase. Therefore, our designed $MoTi_{14}$-based cluster formula (6.25 at.% Mo) is an effective way to define the critical stable solid solutions for these binary, ternary, and multi-component alloys. As summarized in Table 3, the measured Young's modulus from suction casting specimens (SC) of these $[MoTi_{14}]X_1$ (X = Ti, Mo, Nb) alloys are 116, 99, and 92 GPa, respectively. The results after heat treatment are also given. The experimental Young's modulus efficiently decreases with the addition of Nb, similar to previous experimental results on the binary or ternary Ti–Mo–Nb systems. Indeed, for titanium alloys, it is known that Mo is the most effective β stabilizer and Nb is beneficial to reduce the elastic modulus. Based on the above results, it is then confirmed that our modeled composition of $[MoTi_{14}]Nb$ reaches a compromise between low elasticity and high structural stability.

Parallel to experimental measurements, the first-principles calculations based on the cluster-plus-glue-atom and random solid solution models yield a series of Young's moduli that can be compared to experimental data (see Table 3; Fig. 4). For the $MoTi_{14}X_1$ (X = Ti, Mo, Nb) alloys, the random solid solution model yield the Young's moduli of 120–141 GPa for $MoTi_{14}Ti$, 82–122 GPa for $MoTi_{14}Mo$, and even negative values for $MoTi_{14}Nb$. Previously, the first-principles calculations by Raabe et al. [12] also predicted negative values in the region of low Nb (<8 at.%) and Mo (<4 at.%) for the binary Ti alloys with bcc structures. All these results clearly show the general trend that addition of Nb is mechanically unstable and reduces the β stability of Ti–Mo system with the random solid solution structures. Moreover, with different random

Table 2 Alloy compositions of Ti–Mo–Nb alloy series

Alloy series	Cluster formula	Composition (at.%)	Composition (wt%)
$MoTi_{14}X$ (X = Ti, Mo, Nb)	$[MoTi_{14}]Ti$	$Ti_{93.75}Mo_{6.25}$	Ti–11.79Mo
	$[MoTi_{14}]Mo$	$Ti_{87.50}Mo_{12.5}$	Ti–22.26Mo
	$[MoTi_{14}]Nb$	$Ti_{87.50}Mo_{6.25}Nb_{6.25}$	Ti–11.17Mo–10.82Nb
$YTi_{14}Nb_3$ (Y = Ti, Mo)	$[TiTi_{14}]Nb_3$	$Ti_{83.33}Nb_{16.67}$	Ti–27.96Nb
	$[MoTi_{14}]Nb_3$	$Ti_{77.78}Mo_{5.55}Nb_{16.67}$	Ti–9.18Mo–26.68Nb
$MoTi_{15-x}Nb_x$ (x = 1, 2, 3)	$MoTi_{14}Nb$	$Ti_{87.50}Mo_{6.25}Nb_{6.25}$	Ti–11.17Mo–10.82Nb
	$MoTi_{13}Nb_2$	$Ti_{81.25}Mo_{6.25}Nb_{12.5}$	Ti–10.62Mo–20.55Nb
	$MoTi_{12}Nb_3$	$Ti_{75.00}Mo_{6.25}Nb_{18.75}$	Ti–10.11Mo–29.37Nb

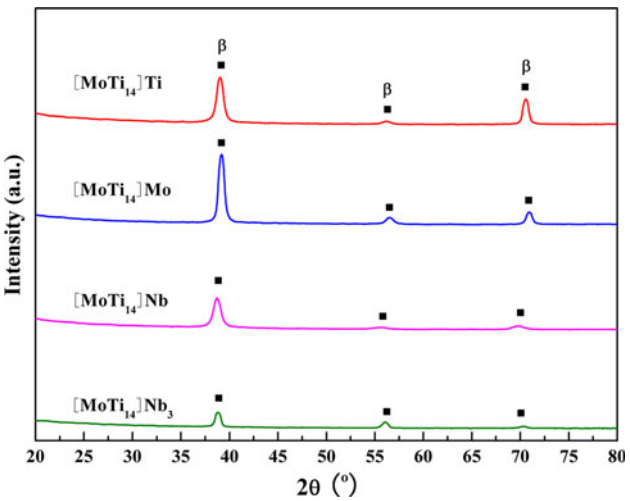

Fig. 3 XRD patterns of Ti–Mo–Nb alloys (Cu $K_{\alpha 1}$ radiation, 40 mA, 40 kV)

structures the calculated Young's modulus could vary seriously by more than 40 GPa.

On the other hand, our structural model on the basis of $[MoTi_{14}]X_1$ cluster formula perfectly maintains the stability of β structure, and the calculated Young's moduli

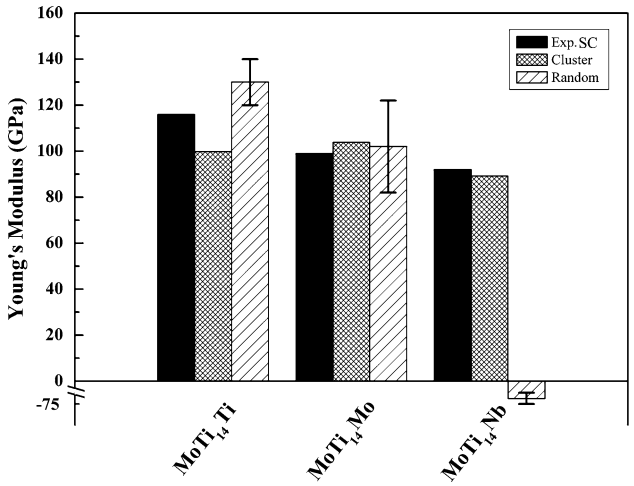

Fig. 4 Young's modulus of $MoTi_{14}X_1$ (X = Ti, Mo, Nb) alloy series. For the $MoTi_{14}Nb$ alloy, the calculated Young's moduli based on the random model are all negative

agree satisfactorily with the experimental values, with an average deviation of only 8 GPa. Further analysis shows that the calculated Young's modulus is mainly determined by the shear modulus. Indeed, the bulk moduli of the two models are quite close to each other; thus the observed differences in Young's modulus from these two models mainly come from the shear modulus, which is more sensitive to the local atomic arrangement.

To further understand the alloying behavior and identify metallurgical trends in Ti–Mo–Nb alloy system with regard to more desired mechanical properties, such as lower Young's modulus, the $[YTi_{14}]Nb_3$ (Y = Ti, Mo) alloys, which also satisfy the cluster-plus-glue-atom model, are examined in the following.

As for Ti–Mo–Nb systems, the measured Young's modulus generally reduces with each increment in Nb content. As shown in Table 3, our measured Young's moduli of these designed $MoTi_{14}$-based alloys are close to the previous experimental results and decrease to 73 GPa for $[MoTi_{14}]Nb_3$ alloy upon further adding Nb content up to 16.67 at.%. Our first-principles calculations also reveal that the Young's modulus of $[MoTi_{14}]Nb_3$ decreases to 83.9 GPa. Thus, appropriately adjusting Nb content in the Ti–Mo–Nb ternary alloys is able to achieve more desirable mechanical properties.

Table 3 Young's modulus and mass density of $[MoTi_{14}]X_1$ (X = Ti, Mo, Nb) and $[YTi_{14}]Nb_3$ (Y = Ti, Mo) alloy series

	$[MoTi_{14}]Ti$	$[MoTi_{14}]Mo$	$[MoTi_{14}]Nb$	$[TiTi_{14}]Nb_3$	$[MoTi_{14}]Nb_3$
$E_{exp(SC)}$ (GPa)	116	99	92		73
$E_{exp(HT)}$ (GPa)	95		82		
E_{theo} (GPa)	99.8	103.8	89.1	83.9	−5.2
ρ_{exp} (g cm^{-3})	4.80	5.29	4.93		5.34
ρ_{theo} (g cm^{-3})	4.75	5.12	5.01	5.23	5.42

The alloy formulated by $[TiTi_{14}]Nb_3$ has not been prepared in our experiments and thus was only investigated by the first-principles calculations. It is interesting to note that $[TiTi_{14}]Nb_3$ (16.67 at.% Nb) alloy exhibits a small negative Young's modulus (−5.2 GPa), implying that the cluster packing structure for $[TiTi_{14}]Nb_3$ alloy is mechanically unstable. Evidently, 16.67 at.% Nb is not enough for complete stabilization of the β phase, which agrees well with the previous experiments that the entire alloy was dominated by α + β phase when 20 at.% Nb was contained and as the Nb content increased to 25 at.%, β phase became the only dominant phase in Ti–Nb binary systems [12]. As for Mo, 6.25 at.% Mo is sufficient to stabilize the same bcc lattice of Ti, suggesting that Mo is even a better β stabilizer than Nb.

To compare with the cluster model, random model within 16-atom supercell was also considered for another series of $MoTi_{15-x}Nb_x$ ($x = 1, 2, 3$) alloys. The calculated Young's modulus is still difficult to draw a definitive conclusion due to the value is significantly affected by the atomic configuration. The calculated Young's moduli of these bcc titanium alloys are negative for a low Nb content of $MoTi_{14}Nb$. For the $MoTi_{13}Nb_2$ composition, the Young's moduli become positive but the calculated elastic constants like C_{44} for some random structures are still negative. Moreover, the calculated Young's moduli with different structures differ by as much as 50 GPa. The relation between the atomic arrangement and Young's modulus is not quite clear. All these results are strikingly opposite to those of the cluster packing structures as well as the experimental data. Again, the present comparison further confirms that the cluster-plus-glue-atom model prevails the random solid solution model used in this study in describing the atomic arrangement and mechanical properties of β-Ti alloys.

From the above discussions, the elastic properties of Mo–Ti–Nb alloy series are well reproduced by the first-principles calculations based on the cluster-plus-glue-atom model for stable solid solution, especially for $MoTi_{14}X_1$ (X = Ti, Mo, Nb) alloy series. This model considers the short-range interaction between solute and solvent elements and can be used as an effective approach to develop new structural biomaterials as shown in our previous work [18]. Essentially, the $MoTi_{14}$ cluster establishes a link between the composition, microstructure, and mechanical properties. Therefore, the cluster formula based on $MoTi_{14}$ cluster provides a useful alloying criterion between low elasticity and high structural stability to develop titanium alloys.

Ductility of $[MoTi_{14}]X_1$ alloys

We further discuss the ductility of $[MoTi_{14}]X_1$ (X = Ti, Mo, Nb) alloy series. As two important quantities to characterize ductility of a material, the ratios of bulk modulus to shear modulus (B/G) and Poisson ratios (v) are listed in Table 4. It is suggested that the transition from brittleness to ductility occurs around a B/G ratio of 1.75 [31]. This critical value does not work for all systems, but serves as a standard to roughly evaluate the tendency of ductility. The B/G ratios obtained for alloys within the cluster-plus-glue-atom structural model are all greater than 1.75, reflecting their ductile characteristics. For the binary compositions of $[MoTi_{14}]Ti$ and $[MoTi_{14}]Mo$, the B/G ratio slightly increases from 2.67 to 2.77. With the addition of Nb, the B/G value suddenly increases to 3.18 (by 19.3 %), as the shear modulus reduces much faster than the bulk modulus. It is thus demonstrated that addition of Nb content effectively improves the ductility of Ti–Mo alloys. Meanwhile, the Poisson ratios show consistent trend but are less sensitive to the alloy compositions with regard to the B/G ratios.

Table 4 Ductility of $MoTi_{14}X_1$ (X = Ti, Mo, Nb) alloy series based on the cluster-plus-glue-atom and random solid solution models

Alloy	Cluster model		Random model	
	B/G	v	B/G	v
$MoTi_{14}Ti$	2.67	0.33	2.09	0.29
$MoTi_{14}Mo$	2.77	0.34	3.26	0.36
$MoTi_{14}Nb$	3.18	0.36	−2.64	0.75

B bulk modulus, G shear modulus, v Poisson ratio

From our tensile experiments, local necking and cone fracture surfaces are observed in the alloy samples, which are typical for the ductile metals. As reported in ref. in [18], the ductility evaluated by elongation and area reduction for $[MoTi_{14}]Nb$ are significantly higher than that of $[MoTi_{14}]Ti$. Therefore, the experimental results at least partially support our theoretical arguments that all these alloys are ductile and the addition of Nb is beneficial for ductility.

On the other hand, the calculated B/G ratios for the random solid solution model are around 2.09, 3.26, and −2.64, and the Poisson ratios are 0.29, 0.36, and 0.75 for the $MoTi_{14}Ti$, $MoTi_{14}Mo$, and $MoTi_{14}Nb$, respectively, without showing any clear correspondence between ductility and alloy compositions. In particular, those theoretical values for the $MoTi_{14}Nb$ composition are totally unreasonable.

According to the above discussions, the calculated ratio of B/G and Poisson ratio illustrate that these parameters are sensitive to shear modulus that is closely related to the local atomic arrangement and is difficult to be precisely reproduced by theoretical simulation as compared with bulk modulus. In this sense, a proper structural model is essential for reliable first-principles calculations and our cluster-plus-glue-atom model indeed reproduces the experimental values satisfactorily.

Electronic structures

In this section, we discuss the electronic structures of β-Ti alloys in terms of their electron density of states and Mulliken populations. Interestingly, even with significant differences in elastic properties, the features of electron DOS from the cluster packing and random structures are nearly identical; thus only those from the cluster model are shown in Fig. 5. Naturally, the electron DOS mainly depends on the local atomic environment. Since the Mo and Nb contents in the alloys are quite low, these solutes atoms are always surrounded by Ti host atoms. Therefore, no matter which model is involved, the local environment seen by the Mo/Nb solute elements is more or less the same, leading to nearly identical electron DOS.

For $[MoTi_{14}]X_1$ (X = Ti, Mo, Nb) alloys, the total DOS always exhibits a pseudogap at Fermi level (see Fig. 5), regardless of the species of the glue atoms or the cluster packing configurations. The overall features of total DOS are dominated by the *d* states of Ti atoms, while the contribution from Mo and Nb is relatively insignificant. In other words, the electronic properties of Ti–Mo–Nb alloys are still mainly determined by the host lattice of bcc Ti. Insensitive to the ratio of glue atoms, the DOS of $[MoTi_{14}]Nb_3$ alloy exhibits basically the same shape.

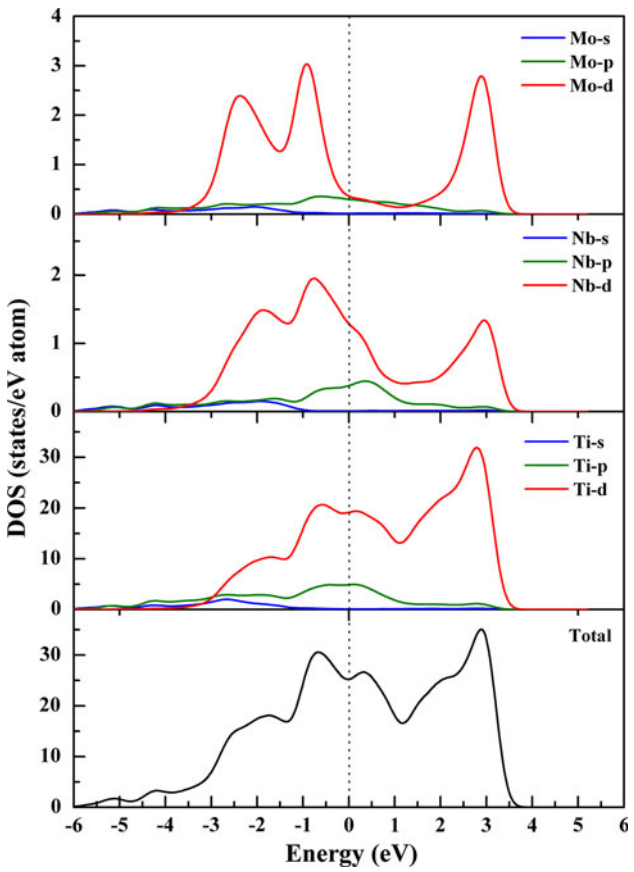

Fig. 5 Total and partial density of states of $[MoTi_{14}]Nb$ alloy described by cluster-plus-glue-atom model

To quantitatively evaluate the charge transfer between different species of atoms, we perform the Mulliken population analysis, which provides rough estimation of partial atomic charges from DFT calculations according to the formalism described by Segall et al. [33]. First of all, the valence electrons transfer from Ti to Mo or Nb, which enhance their half-filled *d* bands. Regardless of the species of glue atoms for $[MoTi_{14}]X_1$ alloys, Mo and Nb atoms of the cluster packing structures gain about 0.62 and 0.38 electrons, respectively, while the amplitudes of charge transfer in the random solid solution structures are slightly lower, i.e., 0.57 and 0.35 electrons for Mo and Nb atoms, respectively. The population analysis on $[MoTi_{14}]Nb_3$ alloy shows that the charge transfer is 0.61 electrons for Mo atoms and 0.33 electrons for Nb atoms, respectively. Such a minor difference implies that the cluster model describes a more stable structure than the random model due to the enhanced charge transfer between the transition metal atoms.

Ashby map

The Ashby map of E/ρ versus B/G [34] is constructed to evaluate the mechanical properties of these Ti–Mo–Nb alloys. The ratio of Young's modulus to density E/ρ, or specific modulus, is an essential engineering parameter to quantify the stiffness of a material per unit weight. Meanwhile, as illustrated above, the ratio of bulk modulus to shear modulus B/G could be used as a standard to measure the ductility.

As shown in Table 3, both experimental and theoretical (within cluster-plus-glue-atom model) mass density of these Ti–Mo–Nb alloys increases linearly with increasing Nb content. The densities derived from the first-principles simulations coincide well with the experimental values with maximum deviation of 5 %, showing the validity of theoretical calculations again.

Previously, Counts et al. [34] showed that stiffness (E/ρ) and ductility (B/G) were inversely correlated for the bcc Mg–Li alloys using ab initio calculations. As shown in Fig. 6, the E/ρ versus B/G curve calculated within the cluster-plus-glue-atom model exhibits the expected feature of contradiction between elasticity and ductility. Specifically, for bcc Ti–Mo–Nb alloys, increasing Nb content up to 16.67 at.% ($[MoTi_{14}]Nb_3$, 26.68 wt%) results in constant reduction in stiffness and enhancement in ductility. On this plot, the least stiff and the most ductile alloy is $[MoTi_{14}]Nb_3$ with a minimum E/ρ value of 15.49 MPa m^3 kg^{-1} and a maximum B/G ratio of 3.55. We expect that further increasing Nb content would still enhance the ductility (as characterized by the B/G ratio), accompanied by a reduction

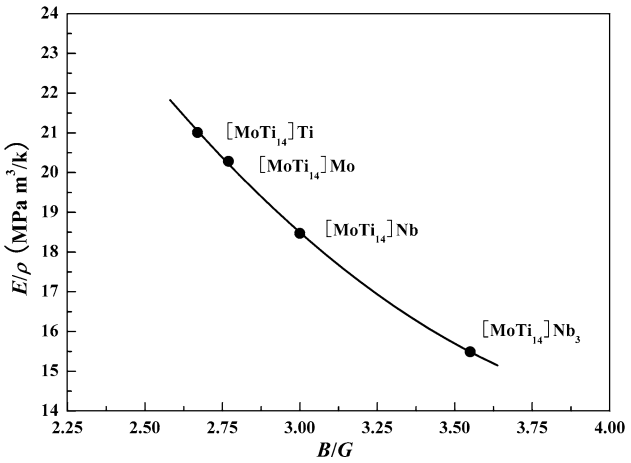

Fig. 6 Ashby map of E/ρ versus B/G for bcc Ti–Mo–Nb alloys (E Young's modulus, ρ mass density, B bulk modulus, G shear modulus). All values are calculated based on the cluster-plus-glue-atom model

in stiffness (described by E/ρ). Therefore, this curve may serve as a useful guide to optimize the composition design of Ti–Mo–Nb alloys.

It is also noteworthy that the first-principles calculations with random solid solution model cannot produce the expected universal master curve. This demonstrates that the random solid solution model is incapable to reflect the substantial connection of alloy properties for β-type Ti–Mo–Nb alloys, whereas the cluster-plus-glue-atom model is confirmed to be a reliable approach to describe and design stable solid solution alloys.

Conclusions

Based on the cluster-plus-glue-atom model for stable solid solution, a series of β-Ti alloys were designed that correspond to the cluster formula of $[MoTi_{14}](\text{glue atom})_x$, where the cluster was the CN14 rhombic dodecahedron polyhedron within bcc lattice and the glue atoms were Mo, Nb, and/or Ti. Using the first-principles calculations, their mechanical properties, especially low Young's modulus, were obtained and compared well with experimental values, while random solid solution models led to erroneous results. These theoretical results validated the cluster-plus-glue-atom model for describing stable β-Ti solid solutions.

The features of electron density of states and Mulliken population were shown to be generally insensible to the atomic configurations. The electronic properties of Ti–Mo–Nb alloys were dominated by the d states from the bcc Ti host lattice, whereas moderate amount of valence electrons transfer from Ti to Mo or Nb, which enhanced their half-filled d bands.

The Ashby map of E/ρ versus B/G constructed according to the cluster models conformed the substantial inverse correlation between stiffness and ductility, which random solid solution models could not reflect. The relevant first-principles calculations demonstrated that the cluster-plus-glue-atom model could be applied to investigate the mechanical properties of β-Ti alloys, especially elastic properties. The present results are useful in guiding industrial alloy composition design. Specifically, for the Ti–Mo based alloys, the composition should be controlled within the Mo/Ti = 1/14 limit to obtain the low elastic modulus alloys with stable β phase.

Acknowledgements The work was financially supported by the National Natural Science Foundation of China (Nos. 51171035, 50901012 and 11174044).

References

1. Bania P (1994) JOM 46(7):16. doi:10.1007/bf03220742
2. Long M, Rack HJ (1998) Biomater 19(18):1621. doi:10.1016/S0142-9612(97)00146-4
3. Ankem S, Greene CA (1999) Mater Sci Eng A 263(2):127. doi:10.1016/S0921-5093(98)01170-8
4. Niinomi M (2003) Sci Technol Adv Mater 4(5):445. doi:10.1016/j.stam.2003.09.002
5. Nag S, Banerjee R, Fraser HL (2005) Mater Sci Eng C 25(3):357. doi:10.1016/j.msec.2004.12.013
6. Wang K (1996) Mater Sci Eng A 213(1–2):134. doi:10.1016/0921-5093(96)10243-4
7. Hao YL, Li SJ, Sun SY, Zheng CY, Hu QM, Yang R (2005) Appl Phys Lett 87(9):091903. doi:10.1063/1.2037192
8. Martins DQ, Osório WR, Souza MEP, Caram R, Garcia A (2008) Electrochim Acta 53(6):2809. doi:10.1016/j.electacta.2007.10.060
9. Xu LJ, Chen YY, Liu ZG, Kong FT (2008) J Alloy Compd 453(1–2):320. doi:10.1016/j.jallcom.2006.11.144
10. Abdel-Hady M, Hinoshita K, Morinaga M (2006) Scr Mater 55(5):477. doi:10.1016/j.scriptamat.2006.04.022
11. Eylon D, Boyer RR, Koss DA (1993) Beta titanium alloys in the 1990s. Minerals, Metals & Materials Society, New York
12. Raabe D, Sander B, Friák M, Ma D, Neugebauer J (2007) Acta Mater 55(13):4475. doi:10.1016/j.actamat.2007.04.024
13. Ikehata H, Nagasako N, Furuta T, Fukumoto A, Miwa K, Saito T (2004) Phys Rev B 70(17):174113. doi:10.1103/PhysRevB.70.174113
14. Hu QM, Lu S, Yang R (2008) Phys Rev B 78(5):052102. doi:10.1103/PhysRevB.78.052102
15. Banerjee R, Nag S, Fraser HL (2005) Mater Sci Eng C 25(3):282. doi:10.1016/j.msec.2004.12.010
16. Dong C, Wang Q, Qiang JB, Wang YM, Jiang N, Han G, Li YH, Wu J, Xia JH (2007) J Phys D Appl Phys 40(15):R273. doi:10.1088/0022-3727/40/15/R01
17. Han G, Qiang JB, Li FW, Yuan L, Quan SG, Wang Q, Wang YM, Dong C, Häussler P (2011) Acta Mater 59(15):5917. doi:10.1016/j.actamat.2011.05.065
18. Ma RT, Hao CP, Wang Q, Ren MF, Wang YM, Dong C (2010) Acta Metall Sin 46(9):1034. doi:10.3724/SP.J.1037.2010.00039
19. Chen JX, Wang Q, Wang YM, Qiang JB, Dong C (2010) Philos Mag Lett 90(9):683. doi:10.1080/09500839.2010.495356
20. Zhang J, Wang Q, Wang YM, Li CY, Wen LS, Dong C (2010) J Mater Res 25(2):328. doi:10.1557/JMR.2010.0041
21. Tian H, Zhang C, Wang L, Zhao JJ, Dong C, Wen B, Wang Q (2011) J Appl Phys 109(12):123520. doi:10.1063/1.3599882
22. Xia JH, Qiang JB, Wang YM, Wang Q, Dong C (2006) Appl Phys Lett 88(10):101903. doi:10.1063/1.2183367

23. Singh J, Singh P, Rattan SK, Prakash S (1994) Phys Rev B 49(2):932. doi:10.1103/PhysRevB.49.932
24. Takeuchi A, Inoue A (2005) Mater Trans JIM 46(12):2817
25. Murray JL (1987) Phase diagrams of binary titanium alloys. ASM International, Materials Park
26. Ho WF, Ju CP, Lin JHC (1999) Biomaterials 20(22):2115. doi:10.1016/s0142-9612(99)00114-3
27. Clark SJ, Segall MD, Pickard CJ, Hasnip PJ, Probert MIJ, Refson K, Payne MC (2005) Z Kristallogr Cryst Mater 220:567. doi:10.1524/zkri.220.5.567.65075
28. Vanderbilt D (1990) Phys Rev B 41(11):7892. doi:10.1103/PhysRevB.41.7892
29. Hammer B, Hansen LB, Nørskov JK (1999) Phys Rev B 59(11):7413. doi:10.1103/PhysRevB.59.7413
30. Hill R (1952) Proc Phys Soc Sect A 65(5):349. doi:10.1088/0370-1298/65/5/307
31. Pugh SF (1954) Philos Mag Ser 7 45(367):823. doi:10.1080/14786440808520496
32. Zunger A, Wei SH, Ferreira LG, Bernard JE (1990) Phys Rev Lett 65(3):353. doi:10.1103/PhysRevLett.65.353
33. Segall MD, Shah R, Pickard CJ, Payne MC (1996) Phys Rev B 54(23):16317. doi:10.1103/PhysRevB.54.16317
34. Counts WA, Friak M, Raabe D, Neugebauer J (2009) Acta Mater 57(1):69. doi:10.1016/j.actamat.2008.08.037